Supporting Information

Kim et al. 10.1073/pnas.1300769110

SI Results

RNAi of *pop-1* (*posterior pharynx defect 1*) and *apr-1* (*adenomatous polyposis coli-related 1*), which are thought to be downstream Wingless/int (Wnt)/β-catenin–related signaling factors, resulted in fully penetrant embryonic lethality but had no affect on WRM-1 (Worm armadillo 1) cortical release (Fig. S1 *A* and *F*). However, in both mutants, WRM-1 nuclear accumulation was significantly reduced (Fig. S2 *A* and *G*), suggesting that these factors promote the nuclear accumulation of WRM-1 downstream of its cortical release. Especially in *apr-1*(*RNAi*), as previously observed (1), the nuclear WRM-1 levels were globally reduced in all cells in the two-, four-, and eight-cell stages, suggesting a general role for APR-1 in WRM-1 nuclear accumulation (Fig. S2*A*). In post-embryonic cells, WRM-1 accumulates in both nuclei of T daughter cells after it is released from the posterior cortex in *apr-1* mutants (2); therefore, APR-1 may have opposite function in terms of nuclear retention of WRM-1 in the endomesoderm (EMS) blastomere and T cells.

RNAi of *glycogen synthase kinase 3* (*gsk-3*) causes cortical retention of WRM-1 as in other upstream Wnt signaling mutants (Fig. 1*C*). However, the interpretation of this phenotype is complicated by the fact that *gsk-3*(*RNAi*) or *gsk-3* deletion allele (*nr2047*) causes an ectopic stabilization of the Oocyte maturation defective 1 gene product, OMA-1 (3). Because WRM-1 is retained on the EMS cortex when OMA-1 is misregulated (Figs. S1 *D* and *F* and S2 *D* and *G*), we cannot exclude the possibility that cortical regulation of WRM-1 by GSK-3 is indirect through stabilized OMA-1 without additional analysis.

1. Nakamura K, et al. (2005) Wnt signaling drives WRM-1/beta-catenin asymmetries in early C. elegans embryos. *Genes Dev* 19(15):1749–1754.
2. Mizumoto K, Sawa H (2007) Cortical beta-catenin and APC regulate asymmetric nuclear beta-catenin localization during asymmetric cell division in C. elegans. *Dev Cell* 12(2):287–299.
3. Shirayama M, et al. (2006) The conserved kinases CDK-1, GSK-3, KIN-19, and MBK-2 promote OMA-1 destruction to regulate the oocyte-to-embryo transition in C. elegans. *Curr Biol* 16(1):47–55.

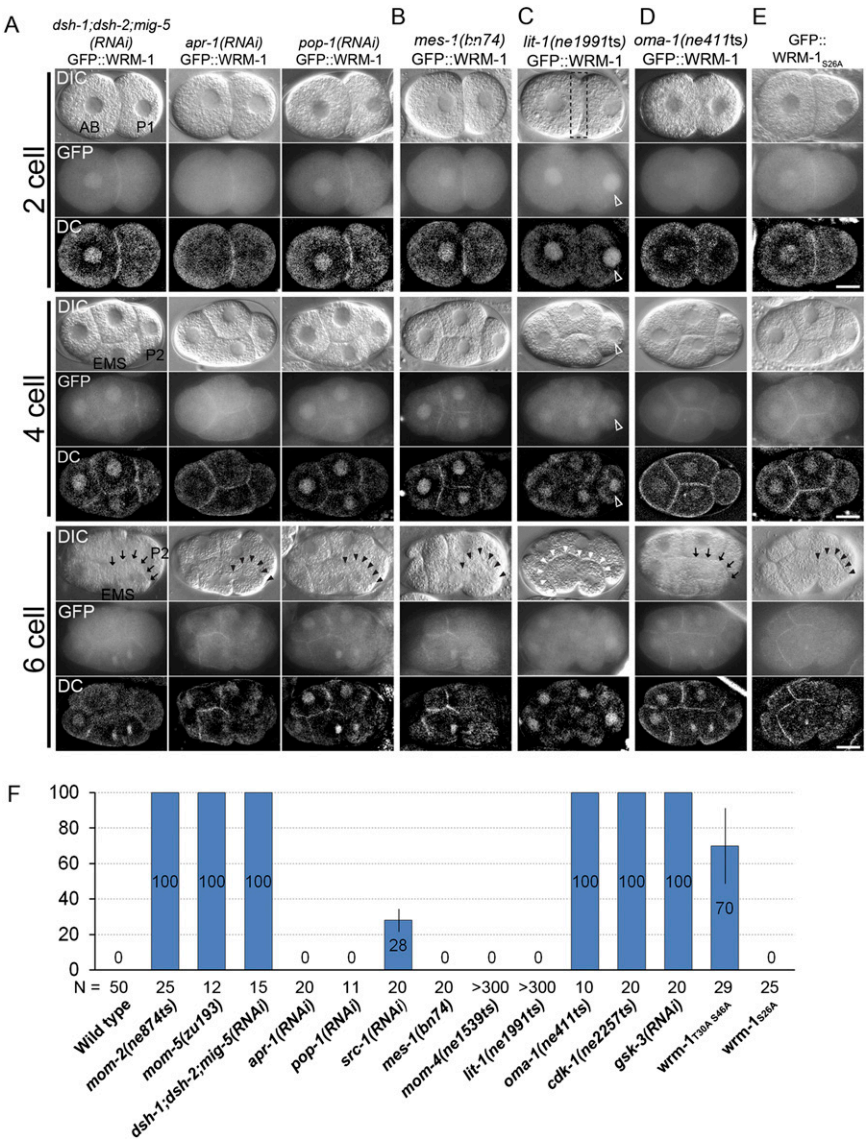

Fig. S1. WRM-1 localization in two-, four-, and six-cell stage embryos. (*A–E*) Nomarski (DIC), fluorescence (GFP), and deconvoluted fluorescence (DC) micrographs of two-, four-, and six-cell stage embryos in the genetic backgrounds indicated. Black arrowheads indicate posterior cortex of dividing EMS cell where the cortical WRM-1 is absent as in WT (Fig. 1*A*). A departure from WT localization pattern is indicated as follows: black arrows, posterior EMS cortex with cortical WRM-1 retention; dotted box, absence of cortical WRM-1 at AB and P1 boundary; empty arrowheads, accumulation of abnormal nuclear WRM-1 in P1 and P2 blastomeres; white arrowheads, entire EMS cortex without cortical WRM-1 localization. Anterior is to the left, and dorsal is up. (Scale bar: 10 μm.) (*F*) Quantification of cortical WRM-1 asymmetry during EMS division. Percentage of embryos that abnormally retain WRM-1 at the posterior cortex during EMS cell division is shown. Genotypes and the number of embryos scored (N) are indicated at the bottom of each bar graph.

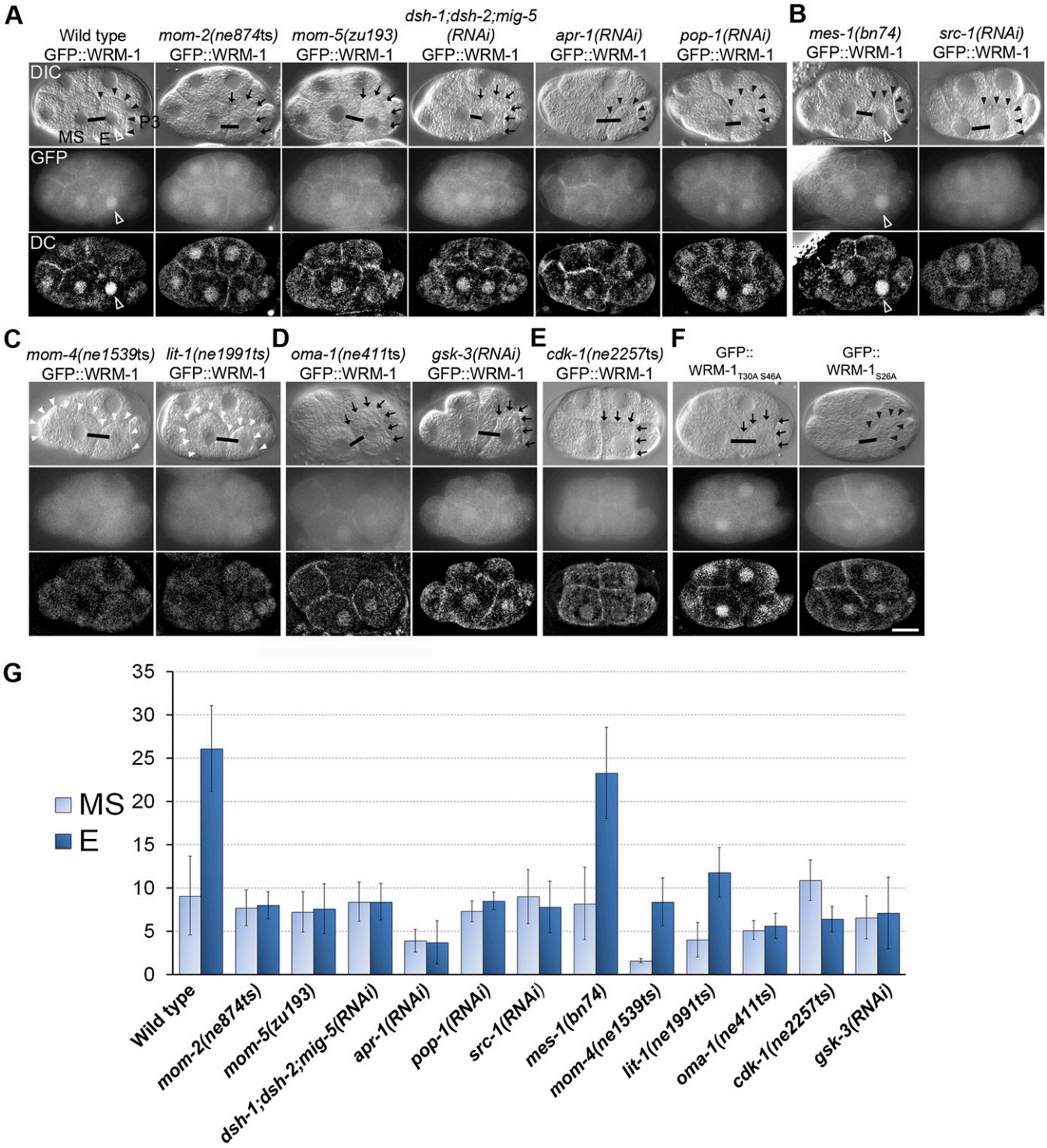

Fig. S2. WRM-1 localization in eight-cell stage embryos. (*A–F*) Nomarski (DIC), fluorescence (GFP), and deconvoluted fluorescence (DC) micrographs of eight-cell stage embryos in the genetic backgrounds indicated. In WT embryos, WRM-1 accumulates to a higher level in the nucleus of E (empty arrowheads) and is absent from the posterior cortex of E (black arrowheads). A departure from the WT localization pattern is indicated as follows: black arrows, WRM-1 is retained at the cortex of E; white arrowheads, WRM-1 is missing from the entire cortex of both E and MS. Black lines connect the nuclei of EMS daughters MS and E. Anterior is to the left, and dorsal is up. (Scale bar: 10 μm.) (*G*) Quantification of nuclear WRM-1 localization in MS and E cells from eight-cell stage embryos. Relative signal intensity of nuclear GFP::WRM-1 in MS and E cells of eight-cell embryos in various genetic backgrounds is shown as indicated. Average signal intensity of 10 embryos from each genotype was analyzed using ImageJ software, in which the nuclear signal value was normalized to the signal in the cytoplasm. Error bars indicate SD.

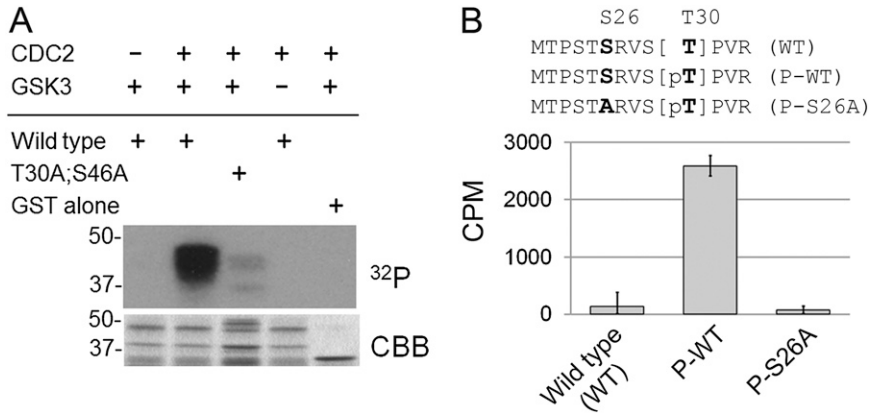

Fig. S3. Sequential phosphorylation of WRM-1 by CDK-1 and GSK-3. (*A*) WT [GST-WRM-1(1-140)], T30A;S46A [GST-WRM-1(1-140) with CDK-phosphoacceptor mutations], or GST alone were incubated first with nonradiolabeled ATP in the presence or absence of human CDC2/cyclin B complex (indicated by CDC2 + or −). After extensive washing, substrates were incubated with γ-[^{32}P]ATP in the presence or absence of vertebrate GSK3β (indicated by GSK3 + or −). Substrates were fractionated by SDS/PAGE and stained with Coomassie Brilliant Blue (CBB). Autoradiography was performed to detect phosphorylation products (^{32}P). (*B*) Recombinant *Caenorhabditis elegans* GSK-3 was used to phosphorylate synthetic WRM-1 peptides encompassing the conserved GSK-3 (S26) and CDK-1(T30) phosphoacceptor sites as indicated with (P-WT) or without (WT) the priming phosphorylation at T30 and with a Ser to Ala mutation at S26 in addition to the priming phosphorylation at T30 (P-S26A).

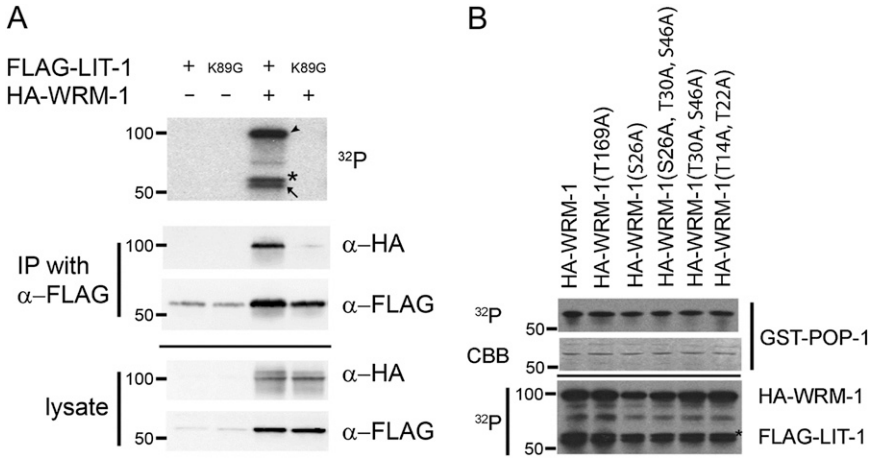

Fig. S4. In vitro LIT-1/WRM-1 kinase assays. (*A*) 293T cells were transfected with FLAG-LIT-1 WT (+) or catalytic mutant (K89G) expression plasmid with or without HA-WRM-1 expression plasmid (+ or −, respectively). FLAG-LIT-1/HA-WRM-1 complexes were immunoprecipitated with α-FLAG M2-agarose beads and assayed for in vitro kinase activity against GST-POP-1(1-188) proteins (*Top*; ^{32}P). The immunoprecipitates (*Middle*; IP with α-FLAG) and lysates (*Bottom*; lysate) were analyzed by Western blotting using α-HA or α-FLAG antibodies as indicated. As reported previously (1), FLAG-LIT-1 alone is an inactive kinase, whereas the FLAG-LIT-1/HA-WRM-1 complex is an active complex that specifically phosphorylates WRM-1 (indicated by the black arrowhead), LIT-1(indicated by the black arrow), and GST-POP-1 (indicated by the asterisk). The FLAG-LIT-1 catalytic mutant (K89G) does not form a stable complex with WRM-1. (*B*) 293T cells were transfected with FLAG-LIT-1 and HA-WRM-1 expression plasmids harboring various mutations affecting phosphorylation sites for GSK-3 (S26), CDK-1 (T30, S46), and potential MAPK sites (T14, T22, and T169). FLAG-LIT-1/HA-WRM-1 complexes were immunoprecipitated with α-FLAG M2-agarose beads and assayed for in vitro kinase activity against GST-POP-1 as in *A*. Phosphorylated GST-POP-1 protein was recovered from the kinase reactions using glutathione beads and analyzed by SDS/PAGE followed by CBB staining (*Middle*) and autoradiography (*Top*; ^{32}P). α-FLAG immunoprecipitates were analyzed for HA-WRM-1 and FLAG-LIT-1 complex formation and autophosphorylation (*Bottom*; ^{32}P). Asterisk indicates carry over GST-POP-1 protein. The formation of the FLAG-LIT-1/HA-WRM-1 complex and its kinase activity was not affected by any of the mutations in WRM-1 that were tested.

1. Rocheleau CE, et al. (1999) WRM-1 activates the LIT-1 protein kinase to transduce anterior/posterior polarity signals in C. elegans. *Cell* 97(6):717–726.

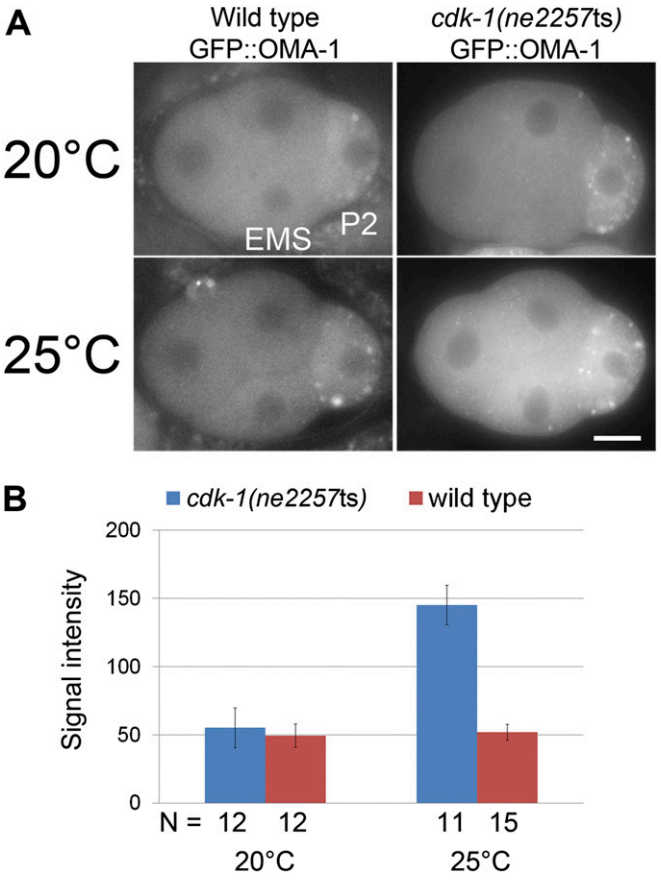

Fig. S5. OMA-1 protein level in four-cell *cdk-1*(*ne2257*ts) embryos. (*A*) Fluorescence micrographs of representative WT and *cdk-1*(*ne2257*ts) four-cell embryos expressing a *gfp::oma-1* transgene (gift from R. Lin) at the nonpermissive temperature (25 °C) or semipermissive temperature (20 °C). Anterior is to the left, and dorsal is up. (Scale bar: 10 μm.) (*B*) Quantification of OMA-1::GFP level was performed using ImageJ software. N, number of embryos scored. Error bars indicate SD.

Table S1. Cortical WRM-1 perturbs proper EMS division orientation

Embryo type	A (%)	B (%)	C (%)	Total *N*
src-1(RNAi)	73.8	16.5	9.7	115
mes-1(bn74)	100.0	0.0	0.0	9
mom-2(RNAi)	95.5	4.5	0.0	22
mom-2(ne834ts)	100.0	0.0	0.0	20
mom-5(RNAi)	94.6	2.7	2.7	37
mom-4(ne1539ts)	100.0	0.0	0.0	10
lit-1(RNAi)	100.0	0.0	0.0	18
lit-1(ne1991ts)	100.0	0.0	0.0	23
wrm-1(RNAi)	100.0	0.0	0.0	47
cdk-1(ne2257ts)	95.7	4.3	0.0	68
cdk-1(ne2257ts); src-1(RNAi)	15.6	20.0	64.4	90
cdk-1(ne2257ts); mom-2(RNAi)	100.0	0.0	0.0	22
cdk-1(ne2257ts); mom-5(RNAi)	100.0	0.0	0.0	15
cdk-1(ne2257ts); src-1(RNAi); lit-1(RNAi)	76.5	5.9	17.6	34
cdk-1(ne2257ts); src-1(RNAi); wrm-1(RNAi)	81.5	11.1	7.4	27
flag::wrm-1;wrm-1(tm514)	100.0	0.0	0.0	45
flag::wrm-1; wrm-1(tm514); mom-4(ne1539ts)	100.0	0.0	0.0	37
flag::wrm-1;wrm-1(tm514);src-1(RNAi)	76.0	22.0	2.0	76
flag::wrm-1; wrm-1(tm514);src-1(RNAi); mom-4(ne1539ts)	74.2	16.1	9.7	31
flag::wrm-1; wrm-1(tm514);src-1(RNAi); wrm-1(RNAi)	71.9	28.1	0.0	32
flag::wrm-1$_{T30AS46A}$; wrm-1(tm514)	100.0	0.0	0.0	46
flag::wrm-1$_{T30AS46A}$; wrm-1(tm514); mom-4(ne1539ts)	100.0	0.0	0.0	11
flag::wrm-1$_{T30AS46A}$; wrm-1(tm514); src-1(RNAi)	30.0	33.3	36.7	68
flag::wrm-1$_{T30AS46A}$; wrm-1(tm514); src-1(RNAi); mom-4(ne1539ts)	75.0	16.7	8.3	36
flag::wrm-1$_{T30AS46A}$; wrm-1(tm514); src-1(RNAi); wrm-1(RNAi)	74.3	22.9	2.8	35
*wrm-1**	100.0	0.0	0.0	10
wrm-1; src-1(RNAi)*	68.0	24.0	0.0	25
wrm-1; wrm-1(tm514)*	100.0	0.0	0.0	30
wrm-1; wrm-1(tm514); src-1(RNAi)*	58.9	38.5	2.6	39
wrm-1$_{T30AS46A}$*	100.0	0.0	0.0	10
wrm-1$_{T30AS46A}$; src-1(RNAi)*	23.0	38.5	38.5	26
wrm-1$_{T30AS46A}$; wrm-1(tm514)*	100.0	0.0	0.0	30
wrm-1$_{T30AS46A}$; wrm-1(tm514); src-1(RNAi)*	40.6	35.1	24.3	37
src-1(RNAi); mom-2(RNAi)	0.0	6.5	93.5	92
src-1(RNAi); mom-2(ne834ts)	15.2	15.2	69.6	33
src-1(RNAi); mom-2(RNAi); mom-4(ne1539ts)	68.2	13.6	18.2	22
src-1(RNAi); mom-2(RNAi); lit-1(ne1991ts)	28.1	46.9	25.0	32
src-1(RNAi); mom-2(ne834ts); wrm-1(RNAi)	64.3	14.3	21.4	28
mes-1(bn74); mom-2(ne834ts)	19.2	23.1	57.7	26
mes-1(bn74); mom-2(RNAi); mom-4(ne1539ts)	60.7	21.4	17.9	28
mes-1(bn74); mom-2(RNAi); lit-1(ne1991ts)	65.6	18.8	15.6	32
mes-1(bn74); mom-2(ne834ts); wrm-1(RNAi)	76.9	9.6	13.5	52

Orientation of EMS mitotic spindle was measured as explained in Fig. 2 and *Materials and Methods*. This table compiles data from Figs. 2 and 4, part of Fig. 5, and additional genetic combinations and controls. Details on the scoring method are in *Materials and Methods*. Phenotypes of some relevant single and double mutants were described in ref. 1.

*Strains expressing *wrm-1* transgenes without an epitope tag (*wrm-1** and *wrm-1*$_{T30AS46A}$*).

1. Bei Y, et al. (2002) SRC-1 and Wnt signaling act together to specify endoderm and to control cleavage orientation in early C. elegans embryos. *Dev Cell* 3(1):113–125.

Table S2. Statistical analysis of the EMS mitotic spindle orientations (multiple-comparisons ANOVA with Bonferroni posthoc analysis)

Category of EMS cell division	RNAi	Population 1	Population 2	*P* value
C	*src-1*	WT	*flag::wrm-1; wrm-1(tm514)*	0.597
C	*src-1*	WT	*flag::wrm-1$_{T30AS46A}$; wrm-1(tm514)*	0.003
C	*src-1*	*flag::wrm-1; wrm-1(tm514)*	*flag::wrm-1$_{T30AS46A}$; wrm-1(tm514)*	<0.001
C	*wrm-1*	WT	*flag::wrm-1; wrm-1(tm514)*	1.000
C	*wrm-1*	WT	*flag::wrm-1$_{T30AS46A}$; wrm-1(tm514)*	1.000
C	*wrm-1*	*flag::wrm-1; wrm-1(tm514)*	*flag::wrm-1$_{T30AS46A}$; wrm-1(tm514)*	1.000
C	*src-1 wrm-1*	WT	*flag::wrm-1; wrm-1(tm514)*	0.001
C	*src-1 wrm-1*	WT	*flag::wrm-1$_{T30AS46A}$; wrm-1(tm514)*	0.045
C	*src-1 wrm-1*	*flag::wrm-1; wrm-1(tm514)*	*flag::wrm-1$_{T30AS46A}$; wrm-1(tm514)*	0.011
B	*src-1*	WT	*flag::wrm-1; wrm-1(tm514)*	0.910
B	*src-1*	WT	*flag::wrm-1$_{T30AS46A}$; wrm-1(tm514)*	0.117
B	*src-1*	*flag::wrm-1; wrm-1(tm514)*	*flag::wrm-1$_{T30AS46A}$; wrm-1(tm514)*	0.271
B	*wrm-1*	WT	*flag::wrm-1; wrm-1(tm514)*	1.000
B	*wrm-1*	WT	*flag::wrm-1$_{T30AS46A}$; wrm-1(tm514)*	1.000
B	*wrm-1*	*flag::wrm-1; wrm-1(tm514)*	*flag::wrm-1$_{T30AS46A}$; wrm-1(tm514)*	1.000
B	*src-1 wrm-1*	WT	*flag::wrm-1; wrm-1(tm514)*	0.185
B	*src-1 wrm-1*	WT	*flag::wrm-1$_{T30AS46A}$; wrm-1(tm514)*	0.164
B	*src-1 wrm-1*	*flag::wrm-1; wrm-1(tm514)*	*flag::wrm-1$_{T30AS46A}$; wrm-1(tm514)*	0.466

P values are reported for multiple comparisons of categories B and C between the strains specified. We used Bonferroni posthoc testing to correct for multiple comparisons.